Experimental Evaluation of the Multiple Friction Pendulum System with Several Sliding Interfaces in Reducing the Seismic Responses of Buildings and Equipments

C. S. Tsai
Department of Civil Engineering, Feng Chia University, Taichung, Taiwan

Y. M. Wang
Graduate Institute of Civil and Hydraulic Engineering, Feng Chia University, Taichung, Taiwan

H. C. Su
Department of Water Resources Engineering and Conservation, Feng Chia University, Taichung, Taiwan

SUMMARY:
This paper presents a performance evaluation of the multiple friction pendulum system (MFPS) with several sliding interfaces on seismic mitigation through a series of shaking table tests with a full scale MFPS-isolated steel building and light weight equipment. In one of the tests, a three-story steel building weighing 40 tons and measuring 3m and 4.5m in two horizontal directions and 9m in height, was equipped with MFPS isolators each with 4 sliding interfaces and subjected to various types of earthquakes to examine the efficiency of the isolators in reducing the seismic response of a structure. Experimental results from the shaking table tests that the roof accelerations, base shears, and column shear forces of the steel structure have been significantly lessened with negligible residual displacements in the isolators when compared to the responses of a fixed-base structure. Furthermore, light weight equipment isolated with MFPS bearings, each with several sliding interfaces, has also been investigated through shaking table tests. Experimental observations demonstrate that the proposed system can greatly reduce the seismic response of equipments. In conclusion, the test results reveal that the MFPS isolation system with several sliding interfaces is an effective tool for protecting both structures and equipments from earthquake damage.

Keywords: Multiple friction pendulum system, seismic isolation, earthquake engineering, equipment

1. INTRODUCTION

The effectiveness of the base isolation technology on seismic mitigation had been proven either from experiment results or earthquake experiences. In the past, a friction pendulum system (FPS) with a single concave sliding surface and an articulated slider, which is a sliding-type isolator, was proposed by Zayas et al. (1987). Through extensive experimental and numerical studies, the FPS isolator has been proven to be an efficient device in reducing the seismic responses of structures (Zayas et al. 1987, Al-Hussaini et al. 1994, Tsai 1997, Jangid 2005). To avoid possibility of resonance of the isolator with long predominant periods of ground motions, an analytical study for a variable curvature friction pendulum system (VCFPS) was conducted by Tsai el al. (2003a). In order to enhance quakeproof efficiency and reduce the size of the FPS isolator, Tsai et al. (2003b, c, 2004, 2005a, b, 2006) proposed a multiple friction pendulum system (MFPS) with double concave surfaces and an articulated slider located between the concave surfaces. In addition, Fenz and Constantinou (2006) conducted follow-up research and published their results. Kim and Yun (2007) reported seismic response characteristics of bridges using the MFPS with double concave sliding interfaces. Furthermore, in 2002, Tsai invented several other types of the MFPS isolator, which basically represent more than one pendulum system, each with multiple sliding interfaces, connected in series (Tsai 2003, 2008). Fenz and Constantinou (2008) conducted research on the characteristics of the MFPS isolator with four sliding interfaces which was invented by Tsai (2003). Morgan and Mahin (2010) investigated the efficiency of the same type of MFPS isolator on seismic mitigation of buildings. In 2009, Tsai et al. revealed the general mechanical characteristic of the MFPS isolator each with numerous sliding interfaces (Tsai et al. 2009a, b, 2010).

In order to further examine the performance of the MFPS isolator with multiple sliding interfaces on seismic mitigation, a series of shaking table tests of a three-story full scale steel structure equipped with the MFPS isolators, each with multiple sliding interfaces, subjected to multidirectional ground motions were carried out at the National Center for Research on Earthquake Engineering in Taiwan. Experimental results demonstrated that the MFPS isolator with multiple sliding interfaces can effectively reduce structural responses during severe earthquakes.

2. PRPPERTIES OF THE MFPS ISOLATION SYSTEM WITH FOUR SLIDING INTERFACES

Figures 2.1 and 2.2 show the exploded and cross-sectional views, respectively, of a MFPS isolator with four sliding interfaces, which includes two subsystems. The first subsystem consists of the sliding interfaces above the articulator and the second subsystem is composed of the sliding interfaces below the articulator. Figures 2.3 and 2.4 show the open-up and cross-sectional views, respectively, of the second subsystem of the MFPS isolator. As shown in Figures 2.3 and 2.4, the MFPS isolator has one spherical concave surface and one intermediate sliding plate below the articulated slider to form two sliding interfaces in the second subsystem. As shown in Figure 2.4, the radii of curvature of the first and second sliding interfaces in the second subsystem are R_1 and R_2, respectively. The friction coefficients of the first, and second sliding interfaces in the second system are μ_1 and μ_2, respectively. The displacement capacities on the 1st and 2nd sliding interfaces are d_1 and d_2 respectively. The radius, friction coefficient, and displacement capacity of each sliding interface of the MFPS isolator is listed in Table 2.1.

3. SHAKING TABLE TESTS OF A THREE-STORY FULL SCALE STEEL STRUCTURE ISOLATED WITH MFPS ISOLATORS EACH WITH FOUR SLIDING INTERFACES

In order to investigate the earthquake-proof efficiency of the MFPS with multiple sliding interfaces subjected to multidirectional excitations, a series of shaking table tests of a three-story full scale steel structure isolated with MFPS isolators, each with four sliding interfaces, were performed at the National Center for Research on Earthquake Engineering in Taiwan. As shown in Figure 3.1, the three-story full scale steel structure was 9 m in height, 4.5 m in length, and 3 m in width, weighing about 40 tons. The dimensions of columns and girders of the steel structure were H200x200x8x12 and H200x150x6x9, respectively. In order to increase the rigidity of the steel structure, diagonal steel bracings (2L100x100x13) were installed on the structure. In the case of the isolated structure, the structure was equipped with four MFPS isolators, one isolator at the bottom of each column. In the tests, the longitudinal direction was defined as the X direction, and the transverse as the Y direction. The fundamental periods of the steel structure in its longitudinal and transverse directions were 0.541 s and 0.275 s, respectively. Acceleration and displacement transducers were installed on each floor during the tests. The input ground motions including the 1940 El Cento earthquake (USA), 1995 Kobe earthquake (Japan), and 1999 Chi-Chi earthquake (TCU068, Taiwan) were given as seismic loads during the shaking table tests. Figure 3.2 shows the picture of the open-up view of the sliding interfaces below the articulated slider of the isolator used for the tests, but the sliding interfaces above the articulated slider are not shown in this figure.

Figures 3.3 to 3.5 show the comparisons of the roof acceleration responses between the fixed-base and isolated-structures in the longitudinal and transverse directions, respectively, while subjected to unidirectional excitations of the El Centro, Kobe, and Chi-Chi earthquakes, respectively. Figures 3.6 and 3.7 compare the roof accelerations between the cases of the fixed-base and isolated structures in the longitudinal and transverse directions, respectively, while subjected to the tri-directional Kobe earthquake, and Figures 3.8 and 3.9 give the comparison of the roof accelerations between the cases of the fixed-base and isolated structures in the longitudinal and transverse directions, respectively, while subjected to the tri-directional Chi-Chi earthquake. These figures tell that the roof accelerations were significantly lessened by installing the MFPS isolators. Figures 3.10 to 3.12 show the comparison of the accelerations between the ground and the base of the superstructure in the longitudinal direction while the system was subjected to unidirectional El Centro, Kobe, and Chi-Chi seismic excitations, respectively. The comparison of the accelerations on the ground and the base of the superstructure in the longitudinal and transverse directions are shown in Figures 3.13 and 3.14, respectively, while subjected to the tri-directional EL Centro earthquake. Figures 3.15 and 3.16 compare the accelerations on the ground and the base of the superstructure in the longitudinal and transverse directions, respectively, while the system was subjected to the tri-directional Kobe earthquake. Figures 3.17 and 3.18 show the comparison of the accelerations on the ground and the base of the superstructure in the longitudinal and transverse directions, respectively, while subjected to the tri-directional Chi-Chi earthquake. The efficiencies of the MFPS in reducing structural vibrations are listed in Tables 3.1 and 3.2. From these results, it can be concluded that the MFPS isolator with four sliding interfaces can significantly reduce structural responses by lengthening the natural period of the entire system, and by providing damping from the frictional force under various types of ground motions. Figures 3.19 and 3.20 show the relative displacement of the MFPS isolator in the longitudinal direction while subjected to uni- and tri-directional ground motions, respectively. It is illustrated from these figures that the MFPS isolator possesses a good restoring mechanism to bring the isolator back to the original position without significant displacements.

4. SHAKING TABLE TESTS OF MOTION SENSITIVE EQUIPMENT WITH MFPS ISOLATORS UNDER MULTI-DIRECTIONAL EARTHQUAKE

In order to examine the earthquake-proof efficiency of the MFPS with multiple sliding interfaces installed in the motion sensitive equipment under tri-directional earthquakes, a series of shaking table tests were performed at the National Center for Research on Earthquake Engineering, Taiwan. As shown in Figure 4.1, the dimensions of motion sensitive equipment is 0.9×0.6×1.94 m, which have six layers inside. A mass of 55 kg at each layer from the first to the fifth layer and 165 kg at the base of the layers was added. The total weights which include the masses and motion sensitive equipment are 608 kg. In the case of the fixed base equipment, the natural frequency was 15.32 Hz. The ground motions of the1995 Kobe and 1999 Chi-Chi earthquakes (TCU068 Station) were given as input excitations in different direction during the shaking table tests.

Figures 4.3 to 4.6 show the comparison between X- and Y-directional acceleration responses at the top layer of the equipment between the fixed base and MFPS isolated systems subjected to tri-directional excitations. From these results, it can be observed that the MFPS isolator with multiple sliding interfaces can significantly reduce seismic responses by lengthening the natural period of the entire system under various types of ground motions.

4. CONCLUSIONS

The characteristics of the multiple friction pendulum system with multiple sliding interfaces are generally functions of radii and friction coefficients of the spherical concave surface and intermediate sliding plates. The natural period and damping effect provided by the MFPS isolator with multiple intermediate sliding plates can change continually during earthquakes. The shaking table test results demonstrate that the proposed MFPS isolator can reduce structural responses significantly without large isolator displacement as a result of considerable damping provided by the isolator and that the MFPS isolator is a promising tool for protection of structures from earthquake damage.

REFERENCES

Al-Hussaini, T. M., Zayas, V. A. and Constantinou, M. C. (1994). Seismic isolation of multi-story frame structures using spherical sliding isolation systems. Technical Report, NCEER-94-0007.

Fenz, D. M. and Constantinou, M. C. (2006). Behaviour of the double concave friction pendulum bearing. *Earthquake Engineering and Structural Dynamics 2006*, **35(11)**, 1403–24.

Fenz, D. M. and Constantinou, M. C. (2008). Spherical sliding isolation bearings with adaptive behavior-theory,

Earthquake Engineering and Structural Dynamics, **37**, 168-183.
Jangid, R. S. (2005). Optimum friction pendulum system for near-fault motions. *Engineering Structures*, **7**, 349-359.
Kim, Y. S. and Yun, C. B. (2007). Seismic response characteristics of bridges using double concave friction pendulum bearings with tri-linear behavior. *Engineering Structures*, **29**, 3082-3093.
Morgan. T. A. and Mahin, S. A. (2010). Achieving reliable seismic performance enhancement using multi-stage friction pendulum isolators. *Earthquake Engineering and Structural Dynamics*, **39**, 1443–1461.
Tsai, C. S. (1997). Finite element formulations for friction pendulum isolation bearings. *International Journal for Numerical Method in Engineering*, **40**, 29-49.
Tsai, C. S. (2003). Improved structures of base isolation systems. Taiwan Patent No. 207126, Publication Number 00542278, Publication Date: July 11, 2003, Application Number 091210175, Filing date: July4, 2002 (in Chinese).
Tsai, C. S., Chiang, T. C. and Chen, B. J. (2003a). Finite element formulations and theoretical study for variable curvature friction pendulum system. *Engineering Structures*, **25**, 1719-1730.
Tsai, C. S., Chiang, T. C. and Chen, B. J. (2003b). Seismic behavior of MFPS Isolated structure under near-fault sources and strong ground motions with long predominant periods. *In The 2003 ASME Pressure Vessels and Piping Conference,* Seismic Engineering, Chen, J. C. (ed.), Cleveland, Ohio, U. S. A., **466**, 73-79.
Tsai, C. S., Chiang, T. C. and Chen, B. J. (2003c). Shaking table tests of a full scale steel structure isolated with MFPS. *In The 2003 ASME Pressure Vessels and Piping Conference, Seismic Engineering*, Chen, J. C. (ed.), Cleveland, Ohio, U. S. A., **466**, 41-47.
Tsai, C. S., Chen, B. J., Pong, W. S. and Chiang, T. C. (2004). Interactive behavior of structures with multiple friction pendulum isolation system and unbounded foundations. *Advances in Structural Engineering, An International Journal*, **7(6)**, 539-551.
Tsai, C. S., Chiang, T. C., Chen, B. J. (2005a). Experimental evaluation piecewise exact solution for predicting seismic responses of spherical sliding type isolated structures. *Earthquake Engineering and Structural Dynamics*, **34(9)**, 1027–1046.
Tsai, C. S., Cheng, C. K., Chen, B. J. and Yu, S. H. (2005b). Experimental study of MFPS-isolated sensitive equipment. *In the 2005 ASME Pressure Vessels and Piping Conference, Seismic Engineering*, ASME, Edited by C. S. Tsai, Denver, Colorado, U.S.A., **8**, 11-18,.
Tsai, C. S., Chen, W. S., Chiang, T. C. and Chen, B. J. (2006). Component and shaking table tests for full-scale multiple friction pendulum system. *Earthquake Engineering and Structural Dynamics 2006*, **35(11)**, 1653–1675.
Tsai, C. S., Lu, P. C., Chen, W. S., Chiang, T. C., Yang C. T. and Lin, Y. C. (2008). Finite element formulation and shaking table tests of direction-optimized friction pendulum system. *Engineering Structures*, **30**, 2321-2329.
Tsai, C. S., Lin, Y. C., and Su, H. C. (2009a). Multiple yield and bounding surfaces model for analysis of multiple friction pendulum system. *In the 2009 ASME Pressure Vessels and Piping Conference, Seismic Engineering*, Paper No. PVP2009-77307.
Tsai, C. S., Lin, Y. C. and Su, H. C. (2009b). Multiple yield and bounding surfaces theory for multiple friction pendulum system. *In the 33rd National Conference on Theoretical and Applied Mechanics*, National United University, Taiwan, Paper No. F2-414.
Tsai, C. S., Lin, Y. C. and Su, H. C. (2010), Characterization and modeling of multiple friction pendulum isolation system with numerous sliding interfaces. *Earthquake Engineering and Structural Dynamics,* **39**, 1463–1491.
Zayas, V. A., Low, S. S. and Mahin, S. A. (1987). The FPS earthquake resisting system Report. EERC Technical Report, UBC/EERC-87/01.

Table 2.1. Dimensions of the MFPS Isolator

Properties of the 1st and 2nd subsystems		
Sliding interfaces	1st and 4th	2nd and 3rd
Radius(m)	2.236	1.50
Period(sec)	3.00	2.457
Minimum friction coefficient	0.047	0.042
Maximum friction coefficient	0.136	0.122
Displacement capacity(mm)	45	70

Table 3.1. Comparisons of Maximum Accelerations Between Fixed-base and MFPS-Isolated Structures in Longitudinal Direction Under Undirectional Excitations

El Centro (PGA X=0.825g)			
Direction	**Ground**	**Isolated-Base**	**Reduction**
NS→X	0.825g	0.306g	62.90%
	Fixed-Roof	**Isolated-Roof**	**Reduction**
NS→X	2.209g	0.313g	85.83%
Kobe (PGA X=0.899g)			
Direction	**Ground**	**Isolated-Base**	**Reduction**
NS→X	0.899g	0.294g	67.33%
	Fixed-Roof	**Isolated-Roof**	**Reduction**
NS→X	3.748g	0.341g	90.91%
Chi-Chi (PGA X=0.730g)			
Direction	**Ground**	**Isolated-Base**	**Reduction**
EW→X	0.730g	0.224g	69.29%
	Fixed-Roof	**Isolated-Roof**	**Reduction**
EW→X	2.055 g	0.325g	84.19%

Table 3.2. Comparisons of Maximum Accelerations Between Fixed-base and MFPS-Isolated Structures in Longitudinal and Transverse Directions Under Tri-directional Excitations

El Centro (PGA X=0.270g, Y=0.424g, Z=0.217g)			
Direction	**Ground**	**Isolated-Base**	**Reduction**
EW→X	0.270g	0.202g	23.49%
	Fixed-Roof	**Isolated- Roof**	**Reduction**
EW→X	N/A	0.219g	N/A
	Ground	**Isolated-Base**	**Reduction**
NS→Y	0.424g	0.172g	59.29%
	Fixed- Roof	**Isolated- Roof**	**Reduction**
NS→Y	N/A	0.198g	N/A
Kobe (PGA X=0.387g, Y=0.285g , Z=0.145g)			
Direction	**Ground**	**Isolated-Base**	**Reduction**
NS→X	0.387g	0.216g	44.22%
	Fixed-Roof	**Isolated-Roof**	**Reduction**
NS→X	1.614g	0.219g	86.43%
	Ground	**Isolated-Base**	**Reduction**
EW→Y	0.285g	0.162g	43.10%
	Fixed-Roof	**Isolated-Roof**	**Reduction**
EW→Y	0.627g	0.166g	73.57%
Chi-Chi (PGA X=0.488g, Y=0.318g, Z=0.456g)			
Direction	**Ground**	**Isolated-Base**	**Reduction**
EW→X	0.488g	0.174g	64.41%
	Fixed-Roof	**Isolated-Roof**	**Reduction**
EW→X	1.280g	0.215g	83.24%
	Ground	**Isolated-Base**	**Reduction**
NS→Y	0.318g	0.134g	57.74%
	Fixed-Roof	**Isolated-Roof**	**Response**
NS→Y	0.564 g	0.170g	69.85%

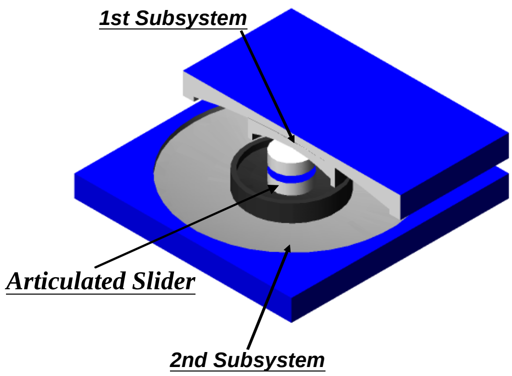

Figure 2.1. Exploded View of The MFPS Isolator With Four Sliding Interfaces

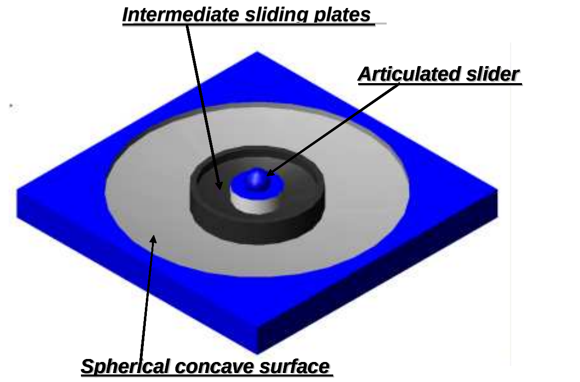

Figure 2.3. Open-up View of The Second Subsystem of The MFPS Isolator With Four Sliding Interfaces

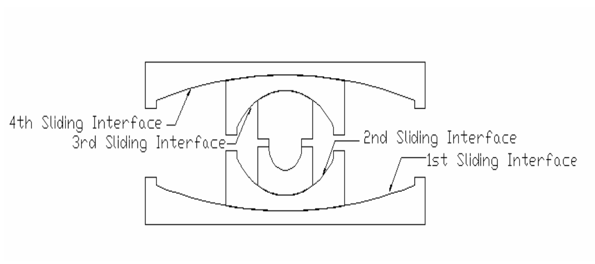

Figure 2.2. Cross-sectional View of The MFPS Isolator With Four Sliding Interfaces

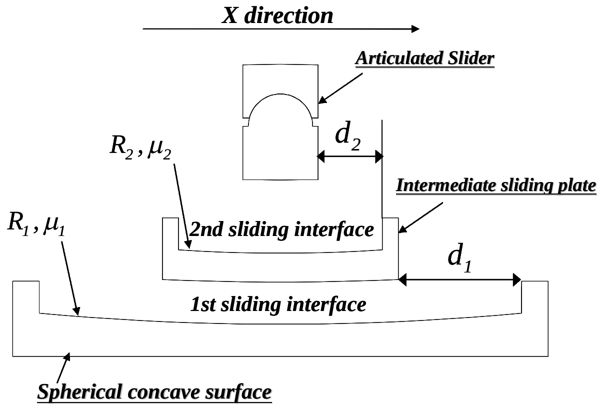

Figure 2.4. Properties of Sliding Interfaces in The Second Subsystem of The MFPS Isolator

Figure 3.1. A Three-story Full Scale Steel Structure

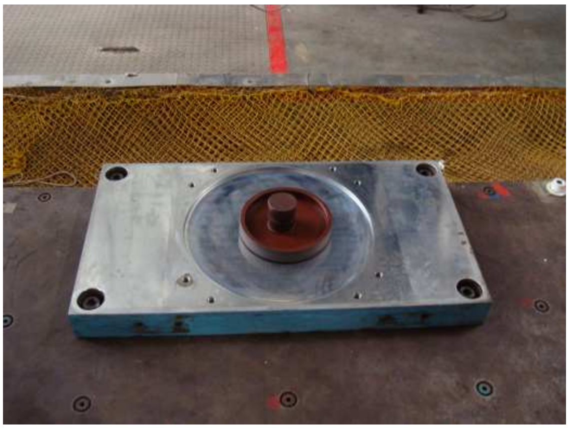

Figure 3.2. Picture For The Open-up View of The Second Subsystem of The MFPS Isolator With Multiple Sliding Interfaces

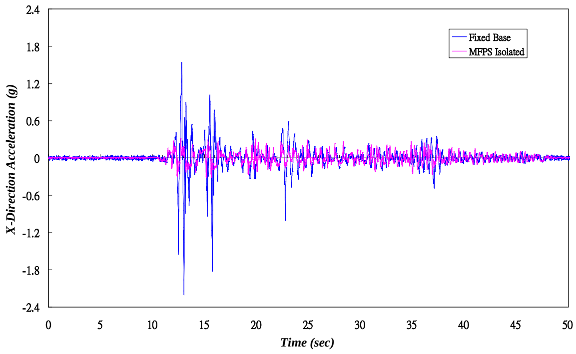

Figure 3.3 Roof Accelerations of Fixed-base and MFPS-Isolated Structures in The Longitudinal Direction Under Uni-Directional EL CENTRO Earthquake (X=0.825g)

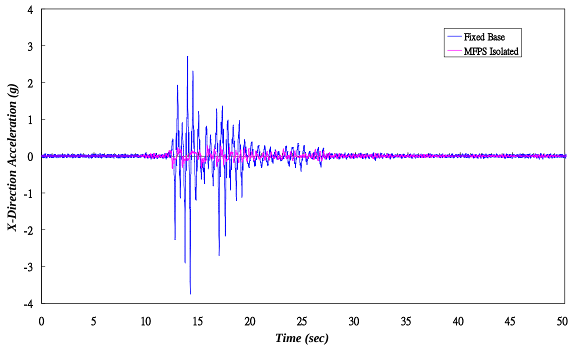

Figure 3.4. Roof Accelerations Response of Structure With Fixed-base and With MFPS Isolated in Longitudinal Direction Under Uni-directional KOBE Earthquake (X=0.899g)

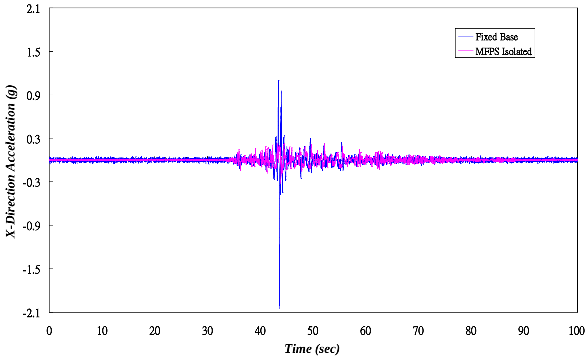

Figure 3.5. Roof Accelerations of Fixed-base and MFPS-Isolated Structures in The Longitudinal Direction Under Uni-Directional CHI-CHI Earthquake, TCU068 STATION (X=0.730g)

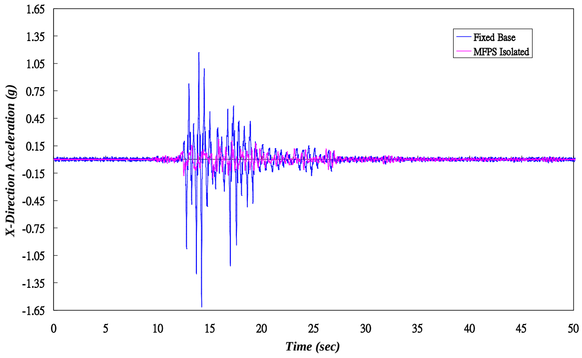

Figure 3.6. Roof Accelerations of Fixed-base and MFPS-Isolated Structures in The Longitudinal Direction Under Tri-Directional KOBE Earthquake (X=0.387g, Y=0.285g, Z=0.145g)

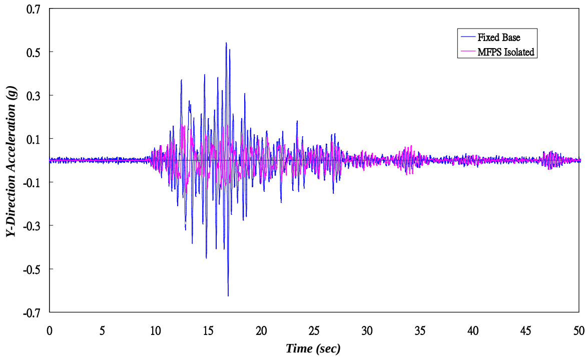

Figure 3.7. Roof Accelerations of Fixed-base and MFPS-Isolated Structures in The Transverse Direction Under Tri-directional KOBE Earthquake (X=0.387g, Y=0.285g, Z=0.145g)

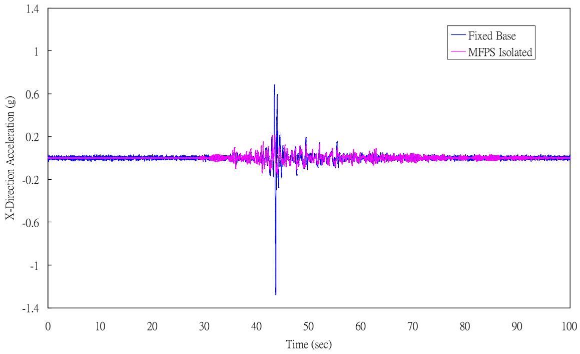

Figure 3.8. Roof Accelerations of Fixed-base and MFPS-Isolated Structures in The Longitudinal Direction Under Tri-directional CHI-CHI Earthquake, TCU068 STATION (X=0.488g, Y=0.318g, Z=0.456g)

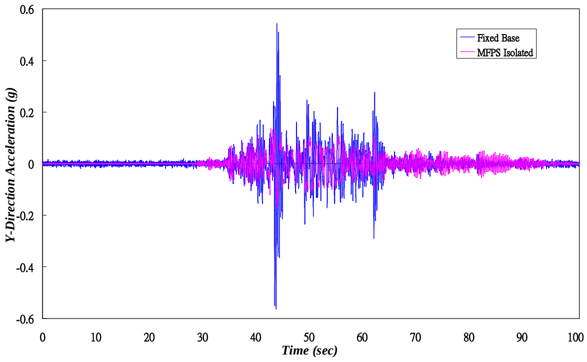

Figure 3.9. Roof Accelerations of Fixed-base and MFPS-Isolated Structures in The Transverse Direction Under Tri-directional CHI-CHI Earthquake, TCU068 STATION (X=0.488g, Y=0.318g, Z=0.456g)

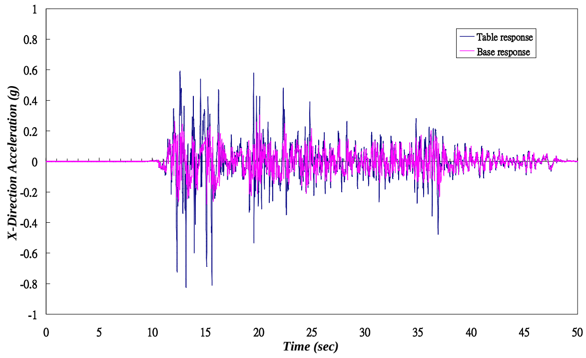

Figure 3.10. Accelerations in The Longitudinal Direction of The Ground and The Base of The Superstructure With MFPS Isolators Under Uni-directional EL CENTRO Earthquake (X=0.825g)

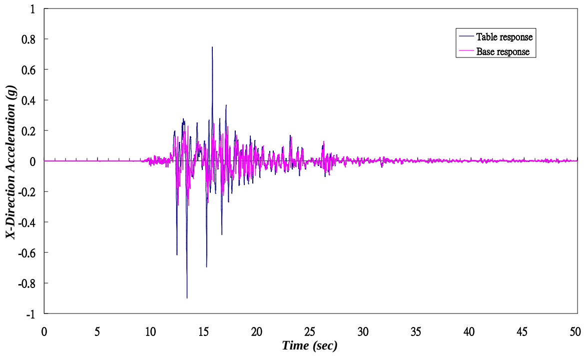

Figure 3.11. Accelerations in The Longitudinal Direction of The Ground and The Base of The Superstructure With MFPS Isolators Under Uni-directional KOBE Earthquake (X=0.899g)

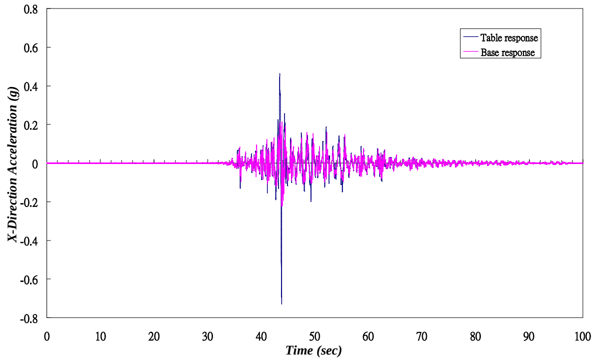

Figure 3.12. Accelerations in The Longitudinal Direction of The Ground and The Base of The Superstructure With MFPS Isolators Under Uni-directional CHI-CHI Earthquake, TCU068 STATION (X=0.730g)

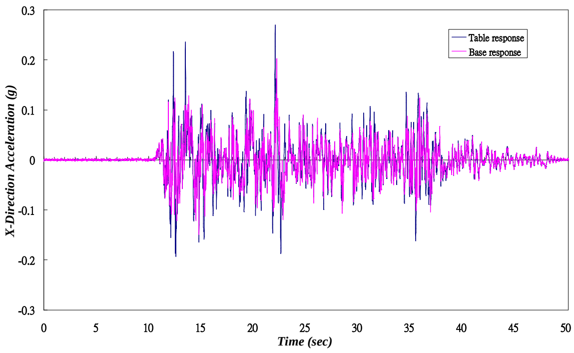

Figure 3.13. Accelerations in The Longitudinal Direction of The Ground and The Base of The Superstructure With MFPS Isolators Under Tri-directional EL CENTRO Earthquake (X=0.270g, Y=0.424g, Z=0.217g)

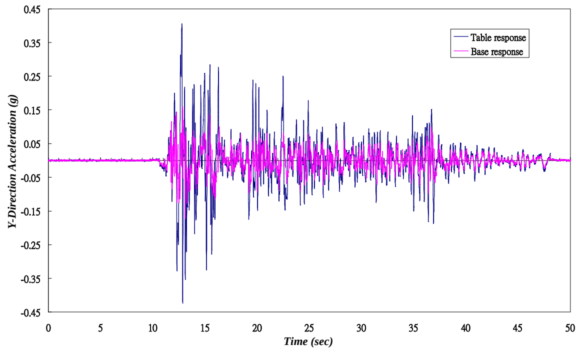

Figure 3.14. Accelerations in The Transverse Direction of The Ground and The Base of The Superstructure With MFPS Isolators Under Tri-directional EL CENTRO Earthquake (X=0.270g, Y=0.424g, Z=0.217g)

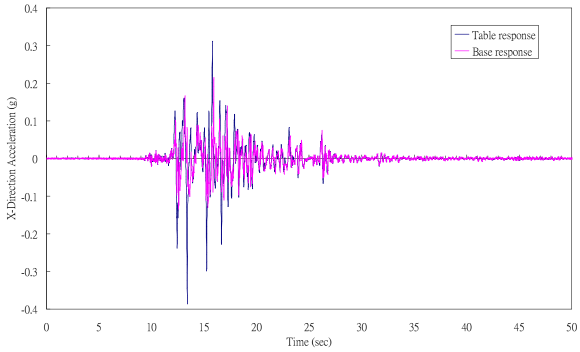

Figure 3.15. Accelerations in The Longitudinal Direction of The Ground and The Base of The Superstructure With MFPS Isolators Under Tri-directional KOBE Earthquake (X=0.387g, Y=0.285g, Z=0.145g)

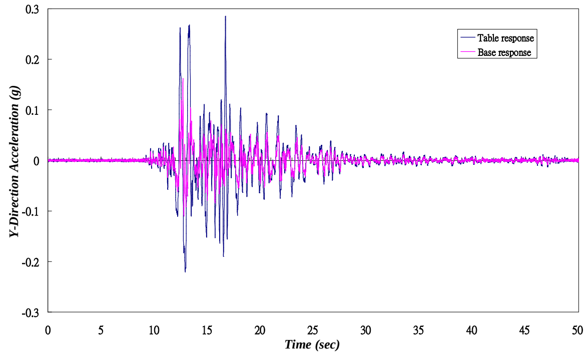

Figure 3.16. Accelerations in The Transverse Direction of The Ground and The Base of The Superstructure With MFPS Isolators Under Tri-directional KOBE Earthquake (X=0.387g, Y=0.285g, Z=0.145g)

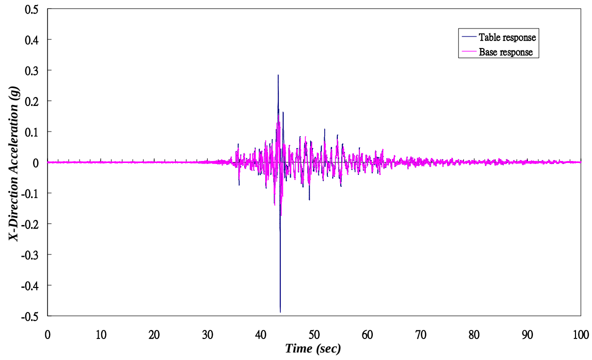

Figure 3.17. Accelerations in The Longitudinal Direction of The Ground and The Base of The Superstructure With MFPS Isolators Under Tri-directional CHI-CHI Earthquake, TCU068 STATION (X=0.488g, Y=0.318g, Z=0.456g)

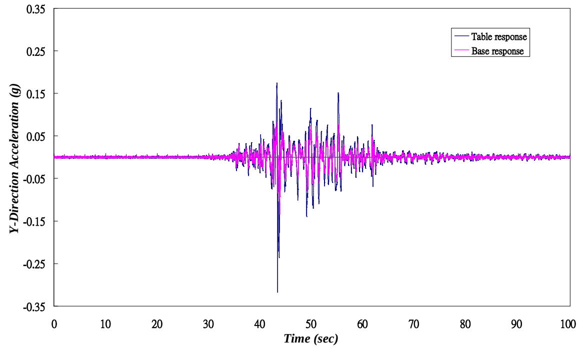

Figure 3.18. Accelerations in The Transverse Direction of The Ground and The Base of The Superstructure With MFPS Isolators Under Tri-directional CHI-CHI Earthquake, TCU068 STATION (X=0.488g, Y=0.318g, Z=0.456g)

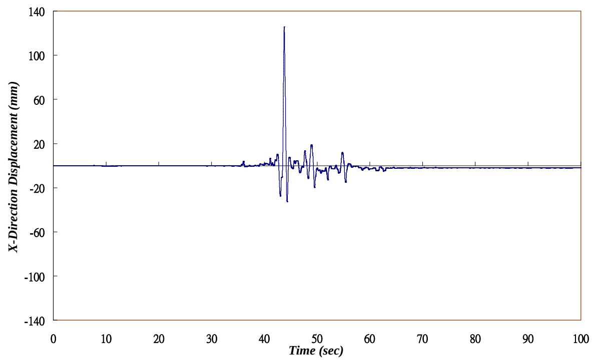

Figure 3.19. Base Isolator Displacement of The MFPS Isolator in The Longitudinal Direction Under Uni-directional CHI-CHI Earthquake, TCU068 STATION (X=0.730g)

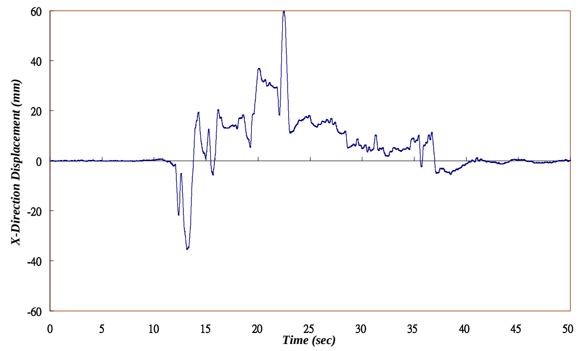

Figure 3.20. Base Isolator Displacement of The MFPS Isolator in The Longitudinal Direction Under Tri-directional EL CENTRO Earthquake (X=0.270g, Y=0.424g, Z=0.217g)

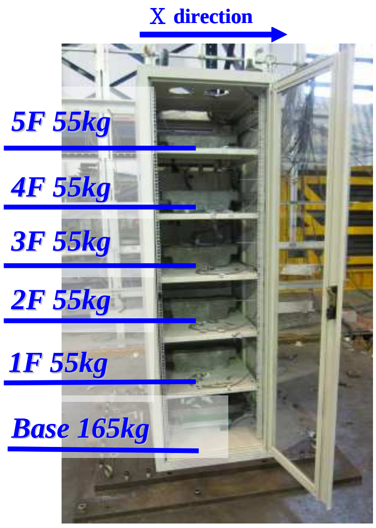

Figure4.1. Motion Sensitive Equipment and Added Masses

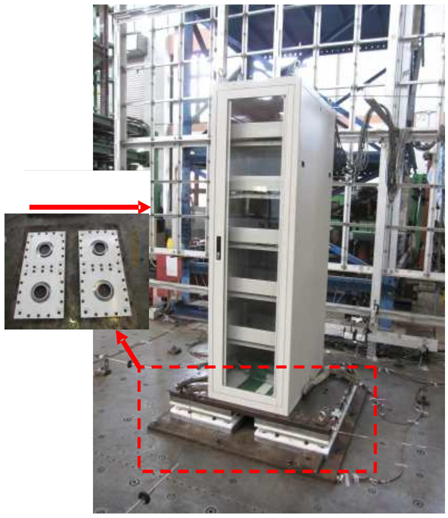

Figure 4.2. Motion Sensitive Equipment Isolated with the MFPS Isolator

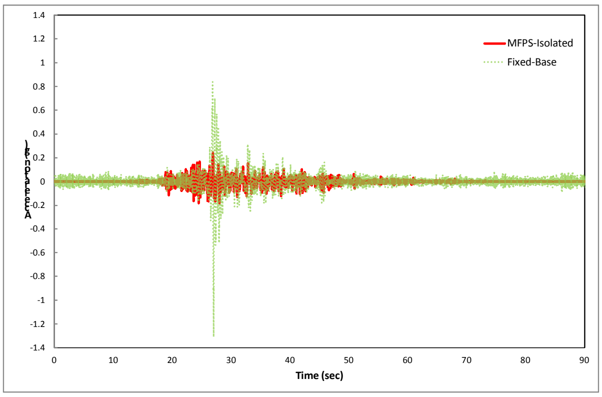

Figure 4.3. Comparison of Top Layer Acceleration of Equipment between Fixed-base and MFPS Isolated System in X-direction under Tri-directional Chi-Chi Earthquake, TCU068 Station (PGA X=0.515g, Y=0.374g, Z=0.474g)

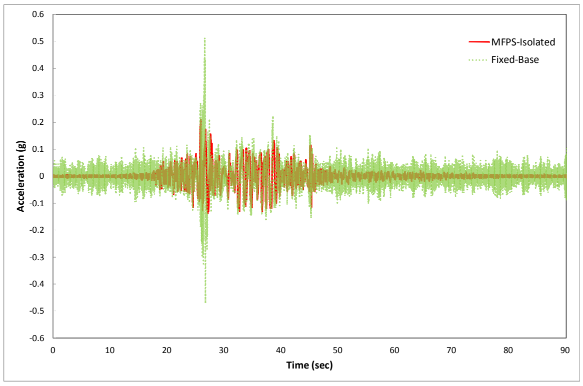

Figure 4.4. Comparison of Top Layer Acceleration of Equipment between Fixed-base and MFPS Isolated System in Y-direction under Tri-directional Chi-Chi Earthquake, TCU068 Station (PGA X=0.515g, Y=0.374g, Z=0.474g)

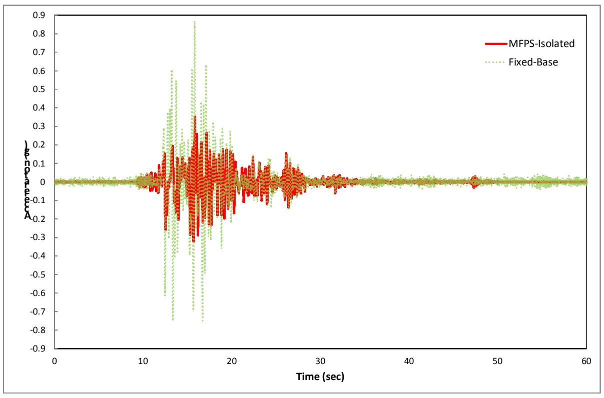

Figure 4.5. Comparison of Top Layer Acceleration of Equipment between Fixed-base and MFPS Isolated System in X-direction under Tri-directional KOBE Earthquake (PGA X=0.382g, Y=0.303g, Z=0.149g)

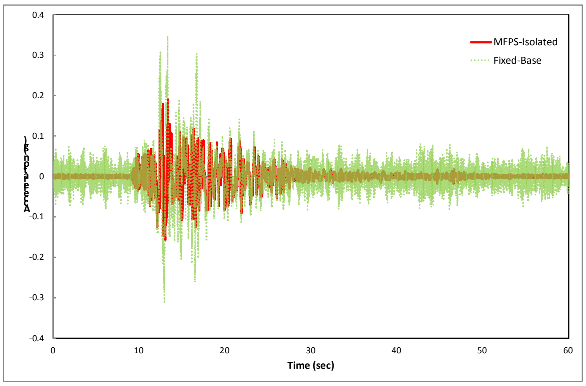

Figure 4.6. Comparison of Top Layer Acceleration of Equipment between Fixed-base and MFPS Isolated System in Y-direction under Tri-directional KOBE Earthquake (PGA X=0.382g, Y=0.303g, Z=0.149g)